Fully Depleted Charge-Coupled Devices

S.E. Holland
LBNL, Berkeley, CA 94720, USA

We have developed fully depleted, back-illuminated CCDs that build upon earlier research and development efforts directed towards technology development of silicon-strip detectors used in high-energy-physics experiments. The CCDs are fabricated on the same type of high-resistivity, float-zone-refined silicon that is used for strip detectors. The use of high-resistivity substrates allows for thick depletion regions, on the order of 200-300 μm, with corresponding high detection efficiency for near-infrared and soft x-ray photons. We compare the fully depleted CCD to the p-i-n diode upon which it is based, and describe the use of fully depleted CCDs in astronomical and x-ray imaging applications.

1. INTRODUCTION

Scientific charge-coupled devices have been used extensively in ground- and space-based astronomy, as well as in other applications. The combination of high detection efficiency, low noise, good spatial resolution, low dark current, and high charge transfer efficiency results in detectors with excellent properties for applications involving the detection of low-light levels [1].

We have developed thick, fully depleted CCDs based on technologies developed for high-energy-physics (HEP) detectors. These CCDs are fabricated on high-resistivity, n-type silicon substrates, and have similarities to the fully depleted p-i-n diode structure that forms the basis of HEP strip and pixel detectors. The use of high-resistivity substrates allows for depletion regions that are 100's of microns in extent. For low-light-level applications the thick depletion regions result in an increase in the quantum efficiency (QE) in the near-infrared portion of the spectrum. Thicker devices also have enhanced detection efficiency for low-energy x rays.

In this work we compare the operating physics of fully depleted CCDs to fully depleted p-i-n diodes, describe unique features of fully depleted CCDs, and describe fabrication technologies under investigation at Lawrence Berkeley National Laboratory (LBNL).

2. P-I-N DIODE AND FULLY DEPLETED CCD COMPARISON

The fully depleted CCD is essentially a p-i-n diode merged with a conventional CCD. Figure 1 shows cross-sectional diagrams of a p-i-n diode, a fully depleted CCD, and a qualitative sketch of the electric field in the high-resistivity, n-type substrate. The electric field plays a key role in the performance of fully depleted CCDs. The electric field versus depth y for the p-i-n diode of Fig. 1 a) is given by

$$E(y) = E_{\max} + \frac{\rho_n}{\epsilon_{\mathrm{Si}}} y \qquad (1)$$

where $E_{\max}$ is the field at the junction of the p^+ and high-resistivity substrate, ϵ_{Si} is the permittivity of silicon, and the volume charge density in the high-resistivity substrate ρ_n is qN_D where q is the electron charge and N_D is the doping density in the substrate. Equation 1 is valid for the case where the p-i-n diode is operated at a substrate bias voltage that exceeds the depletion voltage, *i.e.* overdepleted. From Poisson's equation the slope of the field versus y in Fig. 1 b) is $\rho_n/\epsilon_{\mathrm{Si}}$. $E_{\max}$ is given by

$$E_{\max} = -\left(\frac{V_{\mathrm{sub}}}{y_{\mathrm{sub}}} + \frac{1}{2}\frac{\rho_n}{\epsilon_{\mathrm{Si}}} y_{\mathrm{sub}}\right) \qquad (2)$$

where V_{sub} is the voltage applied to the substrate and y_{sub} is the thickness of the high-resistivity, n-type substrate.

Figure 1 c) shows a cross-sectional drawing of a fully depleted CCD. When compared to the p-i-n structure, it is seen that the p^+ junction of the p-i-n diode has been replaced with a p-type channel region. Bias voltages on polycrystalline silicon gate electrodes over a gate insulator form potential wells and barriers in the p-channel region. A one-dimensional (1D) solution of the Poisson equation for the fully depleted CCD [2] yields an electric field E_J at the p-channel junction to the high-resistivity substrate for the overdepleted case that is given by

$$E_J \equiv -\frac{dV}{dy}(y_J) = -\left(\frac{V_{\mathrm{sub}} - V_J}{y_{\mathrm{sub}}} + \frac{1}{2}\frac{\rho_n}{\epsilon_{\mathrm{Si}}} y_{\mathrm{sub}}\right) \qquad (3)$$

where y_J and V_J are the location of the junction between the p channel and high-resistivity substrate and the potential at that location, respectively. Equation 3 is of the same form as Eq. 2, and therefore the electric field in the high-resistivity substrate of the fully depleted CCD is very similar to that in a fully depleted p-i-n diode.

However, generally speaking CCD pixel sizes are much smaller than the typical pitch in a HEP strip or pixel detector. Because of the strong two-dimensional (2D) effects resulting from the small pixel sizes, the

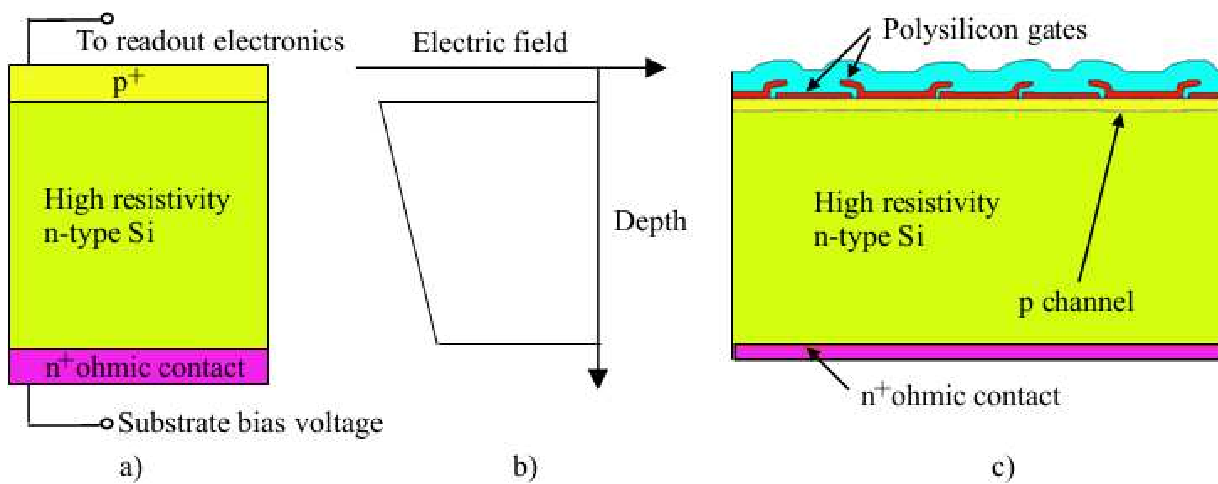

Figure 1: a) Cross-sectional diagram of a p-i-n diode. b) Qualitative sketch of the electric field in the high-resistivity, n-type silicon for the case when the diode and CCD are operated in the overdepleted condition. c) Cross-sectional diagram of a fully depleted CCD.

fields and potentials in a fully depleted CCD will deviate significantly from the 1D model near the CCD potential wells [2]. Also, in the fully depleted CCD an electric field of opposite sign to that in the substrate is present in the CCD channel. Nonetheless, the fully depleted CCD benefits significantly from features common with the basic p-i-n diode used in high-energy physics. As shown later the ability to fully deplete thick devices extends the useful wavelength sensitivity of the CCD to near-infrared wavelengths. The use of a fully depleted structure also results in a well controlled spatial resolution that can be improved by operating at high substrate bias voltages.

Inherent properties of CCDs allow for some performance advantages when compared to HEP p-i-n detectors. Charge collected in CCD pixels is transferred in a noise-less fashion to a low capacitance on-chip amplifier, resulting in a large charge to voltage conversion factor, about 3.5 μV/e$^-$ for the CCDs described here. This in conjunction with double correlated sampling signal processing, which was invented for CCDs [3], results in excellent noise performance for devices operated in slow scan mode. The CCDs described in this work have noise levels of about 3–4 e$^-$ rms at readout speeds of 70 kpixels/sec, and noise levels approaching 1 e$^-$ have been reported by others.

However, CCDs usually have a limited number of output amplifiers, typically 2–4, in contrast to the large number of readout channels for a HEP strip or pixel detector. Fully depleted CCDs would benefit from advances in massively parallel readout as is done in HEP experiments. Development of massively parallel readout would address the major shortcoming of scientific CCDs, which is the slow readout speed.

Finally, CCDs and p-i-n diodes differ significantly in terms of fabrication complexity. A single-sided, DC-coupled strip detector can be fabricated with as few as 3 photomasks. AC-coupled detectors with polycrystalline silicon bias resistors add 1–2 photomasks, and the number of photomasks required is doubled for double-sided detectors.

The CCD process used in this work requires 11 photomasks and uses three layers of polycrystalline silicon to form the 3-phase clocking structure. The polycrystalline silicon gates overlap for efficient charge transfer, and the overlapping layers are isolated by thermally grown layers of SiO_2. As a result there are numerous high temperature steps in a CCD process, and care is required to maintain low dark current especially when high-resistivity substrates are used. We employ an in-situ doped (phosphorus) polycrystalline silicon layer on the backside of the wafer for gettering of transition metals that would otherwise form mid-gap states in the silicon bandgap and degrade the dark current [4]. This technique has been demonstrated to maintain low dark currents even after processing steps exceeding 8 hours at 1000°C. Figure 2 shows a 100 mm diameter wafer with a single-sided strip detector fabricated at LBNL and a 150 mm diameter wafer containing fully depleted CCDs.

3. UNIQUE FEATURES OF FULLY DEPLETED CCDS

The ability to operate thick CCDs fully depleted has several advantages. Figure 3 compares measured quantum efficiency of a 250 μm thick, fully depleted CCD with a 10–20 μm thick device. In addition, the absorption length of silicon at -100 and -120°C is also shown in Fig. 3.

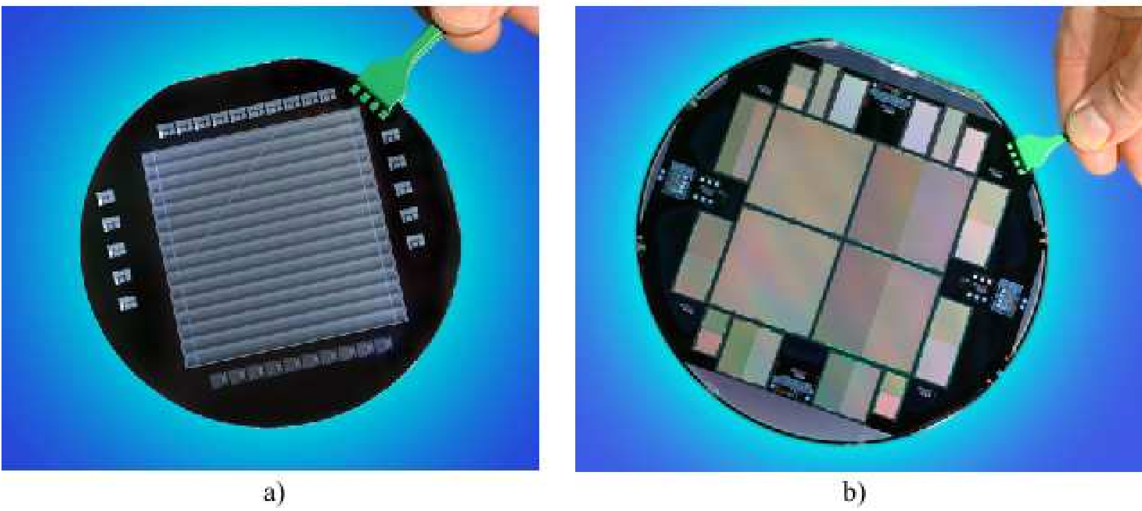

Figure 2: a) 100 mm diameter wafer containing a large area, single-sided silicon strip detector fabricated at LBNL. b) Fully depleted CCDs fabricated at DALSA Semiconductor on 150 mm diameter wafers. The 4 large CCDs are 3512^2 devices with 10.5 μm pixels.

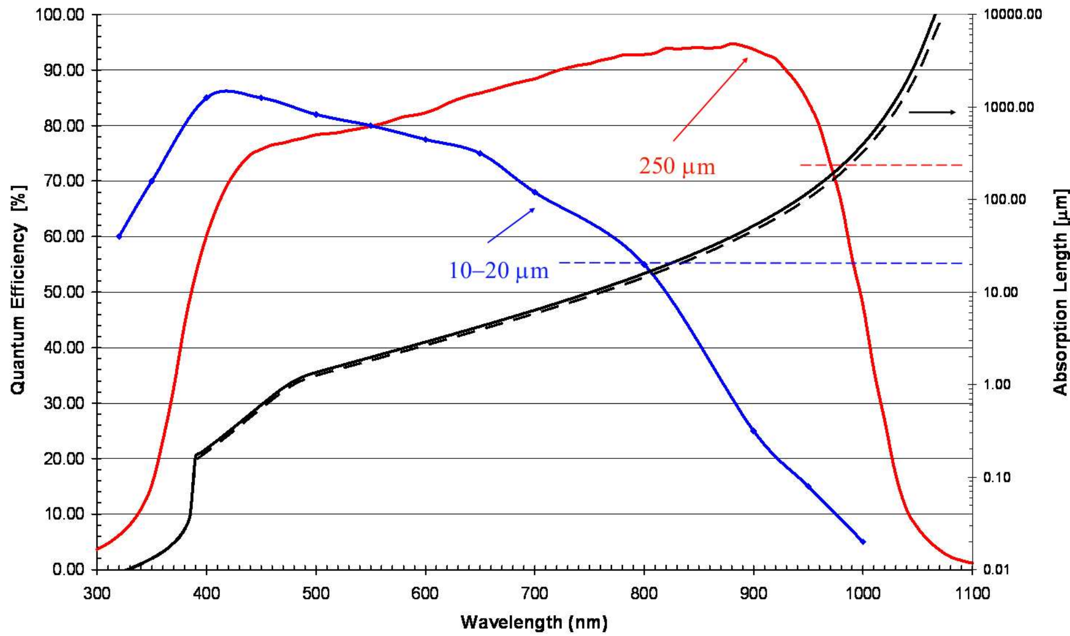

Figure 3: Measured quantum efficiencies of a 250 μm thick, fully depleted CCD and a 10–20 μm thick, partially depleted CCD. Also shown in the absorption length in silicon for temperatures of -100 and -120°C. The dashed lines correspond to the CCD thickness.

At photon energies less than about 2.5 eV silicon is an indirect bandgap material. Phonons are required for momentum conservation when light is absorbed, and as a result the absorption process becomes inefficient in the indirect bandgap regime, corresponding to wavelengths larger than about 500 nm. This is seen in the absorption length curves in Fig. 3 where it is noted that the absorption length is hundreds of microns in the near-infrared region. The steep rolloff of the QE starting at about 950 nm for the fully depleted CCD is due to the strongly increasing absorption length, which exceeds the CCD thickness at about 970 nm. At wavelengths larger than that corresponding to the bandgap the CCD becomes transparent, neglecting free-carrier absorption effects that are only important in heavily doped regions.

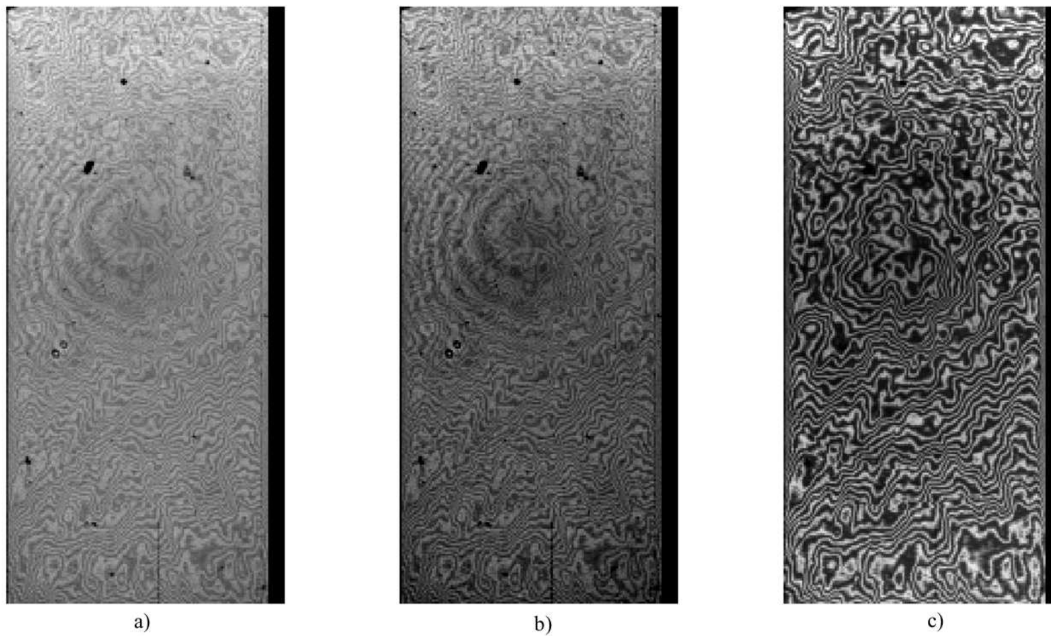

Figure 4: Uniform illumination of a thinned, back-illuminated CCD. at wavelengths of a) 800 nm, b) 900 nm and c) 1000 nm. The CCD is 10–20 μm thick. Measurements courtesy of Richard Stover, University of California Observatories.

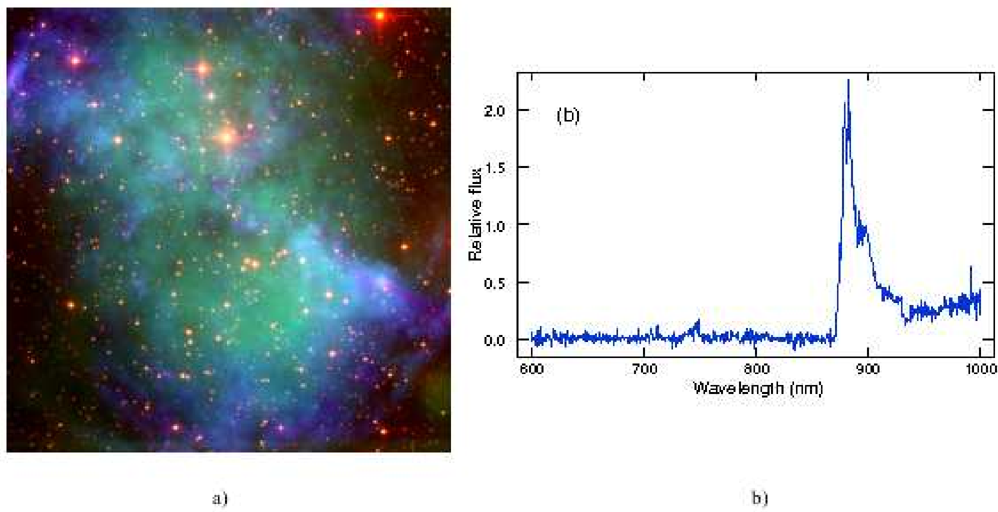

Figure 5: a) False color image of the Dumbbell nebula taken with a fully depleted, back-illuminated CCD [5]. b) Spectrum of a high redshift quasar taken with a fully depleted, back-illuminated CCD [6]. Results courtesy of the National Optical Astronomy Observatory and the WIYN Observatory.

Figure 3 demonstrates the enhancement in near-infrared quantum efficiency that results when the CCD thickness is increased. Although the thinned device still responds at wavelengths where the absorption length exceeds the CCD thickness, multiply-reflected light results in interference fringes. Shown in Fig. 4 are the results of the uniform illumination of a thinned, back-illuminated CCD at wavelengths of 800, 900 and 1000 nm. The large amplitude fringing seen at long wavelengths complicates the use of thinned CCDs at near-infrared wavelengths.

Figure 5 shows results from astronomical imaging and spectroscopy at the National Optical Astronomy Observatory (NOAO) for approximately 300 μm thick CCDs produced at LBNL. Figure 5 a) shows a false color image of the Dumbbell Nebula generated from images taken with three filters. The blue and green correspond to narrow-band filters at the H-α wave-

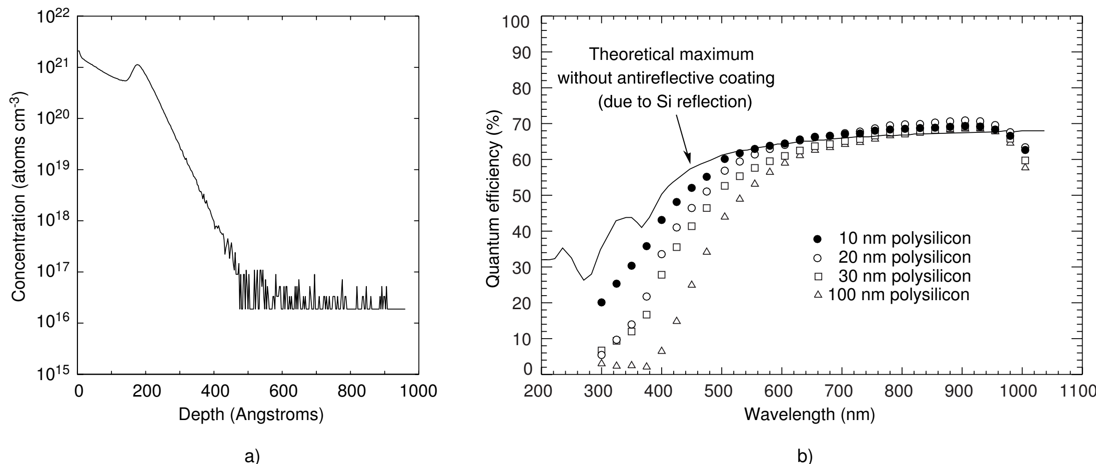

Figure 6: a) Secondary ion mass spectrometry measurement of the phosphorus concentration versus depth for an ≈ 20 nm in-situ doped (phosphorus) polycrystalline silicon film deposited on high-resistivity silicon. b) Measured quantum efficiencies for back-illuminated photodiodes with varying thickness in-situ doped (phosphorus) polycrystalline silicon films deposited on the back side of the high-resistivity silicon substrate [7].

length of 650 nm and the [SIII] line at 953 nm, respectively. An intermediate-band filter centered at approximately 1.0 μm corresponds to red in the image. Figure 5 b) shows the spectrum of a high redshift quasar, also measured at NOAO. The Lyman-α peak has been redshifted from the UV to the near infrared. The measurements shown in Figure 5 would not be practical with the thinned CCDs whose properties are shown in Figs. 3 and 4 due to the low quantum efficiency and significant fringing that are characteristic of thinned, back-illuminated CCDs.

In addition to good near-infrared response, it is important to have high QE in the blue end of the spectrum as well. Figure 3 shows that the absorption length in the blue is very small, about 0.1 μm at 400 nm and even smaller at shorter wavelengths. In order to detect blue light efficiently the ≈ 1 μm thick polycrystalline silicon gettering layer [4], which is essentially opaque below about 500 nm, is removed near the end of the process sequence and replaced by a much thinner, in-situ doped (phosphorus) polycrystalline silicon layer [2, 7]. In addition, anti-reflection coatings are used to minimize reflection losses and further enhance the QE. Figure 6 a) shows the phosphorus concentration versus depth as measured by secondary ion mass spectrometry for an ≈ 20 nm thick layer of in-situ doped polycrystalline silicon deposited on a high-resistivity silicon substrate. Figure 6 b) shows quantum efficiency versus wavelength measured on photodiodes for various thickness backside polycrystalline silicon layers [7].

Fully depleted CCDs have a spatial resolution that is controlled by the device thickness, operating temperature, and substrate bias voltage [2]. The latter effect is shown in Fig. 7, which shows the measured charge distribution for a point source illumination [8]. At the lowest substrate bias voltage the CCD is not fully depleted and the spatial resolution is degraded by diffusion of the photogenerated holes in the undepleted region [2]. Increasing the substrate bias voltage to 20V is sufficient to fully deplete the CCD. Once fully depleted the spatial resolution depends on the lateral diffusion of the photogenerated holes during their transit to the CCD collection wells. While much improved over the 5V case, the measured point-spread function (PSF) is 9.1 μm rms, which is too large for some applications. Increasing the substrate bias voltage to 115V results in a PSF of 3.7 μm. At this level of PSF small pixel CCDs can be contemplated, and in fact the CCD used to generate the data of Fig. 7 has 10.5 μm pixels. At the 20V substrate bias voltage the PSF is comparable to the pixel size, and in that case the effective pixel size due to carrier diffusion exceeds the actual pixel size.

The operation of fully depleted CCDs at high substrate bias voltages offers significant challenges in terms of device design. The CCD pixel includes a buried channel, a gate insulator, and a polycrystalline gate electrode. The gate insulator is typically ≈ 100 nm thick and usually consists of a stack of SiO_2 and Si_3N_4 [1]. The dielectric breakdown voltage of such a layer is in the 80–100 V range, and therefore care must be taken in the device design to ensure that potentials in this range cannot be impressed across the gate insulator when using high substrate bias voltages.

In addition, CCDs have channel-stop regions that are somewhat analagous to implanted regions that are used to block inversion layers that naturally form at Si-SiO_2 interfaces on high-resistivity, p-type silicon [9]. In the CCD case the channel stops must be biased when high substrate bias voltages are used, and a significant part of the device design effort is devoted

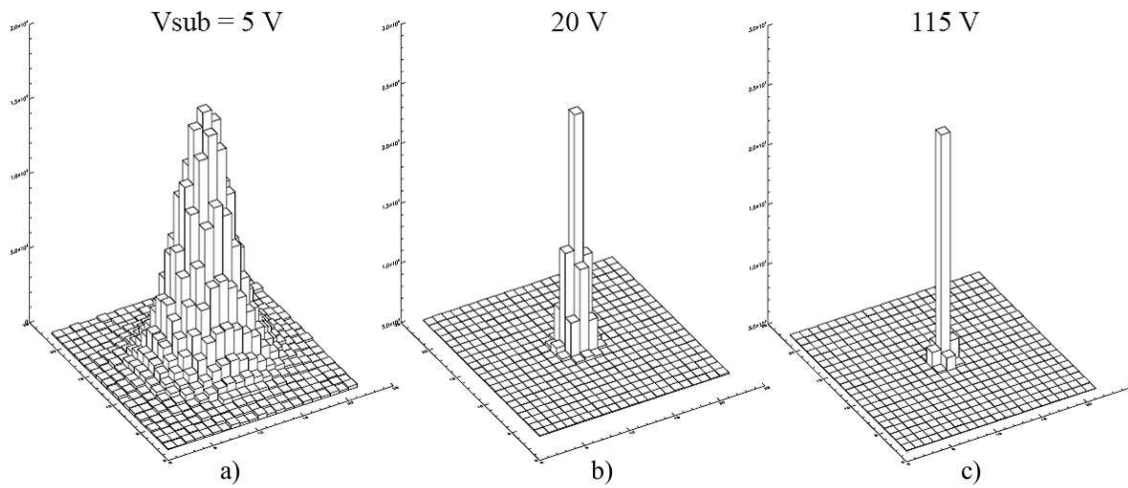

Figure 7: Measured charge distribution resulting from back illumination using a pinhole projector with a small spot size of ≈ 2 μm rms. Each square represents the measured charge for a 10.5 μm pixel. a) $V_{\rm sub}$=5V. The CCD is not fully depleted. b) $V_{\rm sub}$=20V. The CCD is just fully depleted and the measured PSF is 9.1 μm rms. c) $V_{\rm sub}$=115V. The CCD is overdepleted and the measured PSF is 3.7 μm [8].

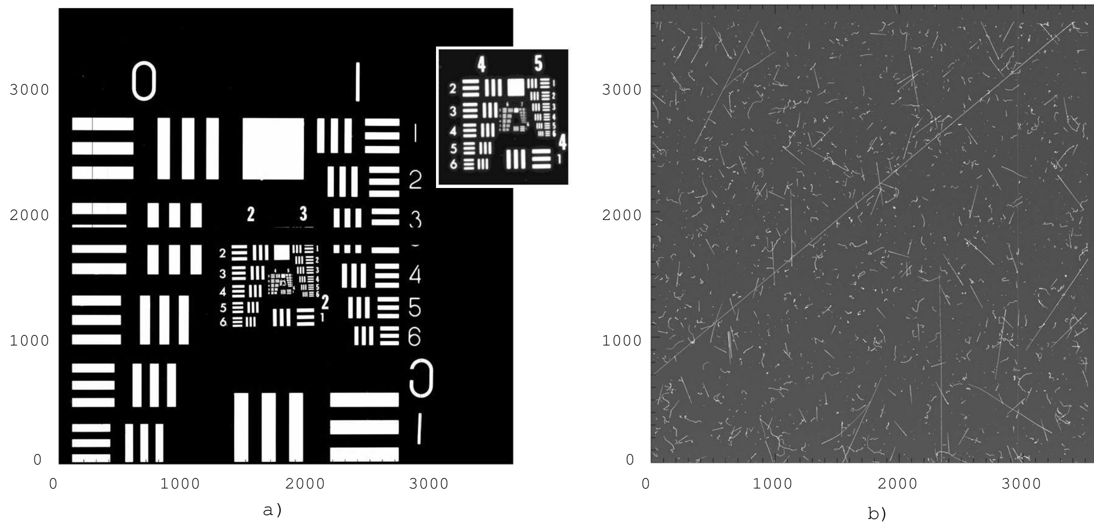

Figure 8: a) Test pattern image taken on a 3512^2, 10.5 μm pixel back-illuminated CCD. The substrate bias voltage was 206V, and the operating temperature was -140° C. The inset is a magnified view of the smallest test patterns. b) 30 minute dark exposure for a ≈ 650 μm thick, 3512^2, 10.5 μm pixel CCD at a substrate bias voltage of 206V. The background is due to cosmic rays and Compton electrons from terrestrial radiation. The dark current was 0.63 electrons/pixel-hour at -140° C.

to the channel-stop regions [10].

We have developed high-voltage-compatible CCDs that can be operated at substrate bias voltages of at least 200 V. Figure 8 shows results from the operation of 200 and 650 μm thick CCDs at substrate bias voltages of 206V [10]. Figure 8 a) shows a test pattern image taken on a 200 μm thick, back-illuminated CCD while Fig. 8 b) shows results for a 650 μm thick CCD. The latter is the result of a 30 minute integration under dark conditions. The lack of PSF degradation on the tails of the cosmic ray and background radiation events implies full depletion of this thick CCD at a substrate bias voltage of 206V.

The ability to fully deplete thick devices extends the x-ray response for silicon CCDs. A 200 μm thick CCD is essentially 100 % efficient for the detection of 8 keV x rays, and a 650 μm device has 50 % efficiency for 20 keV x rays [11]. Figure 9 shows x-ray imaging results with a fully depleted, 200 μm thick CCD of a stainless-steel target and phantoms embedded in paraffin using 8 keV x rays from a Cu anode [10].

A significant issue for the direct detection of x rays

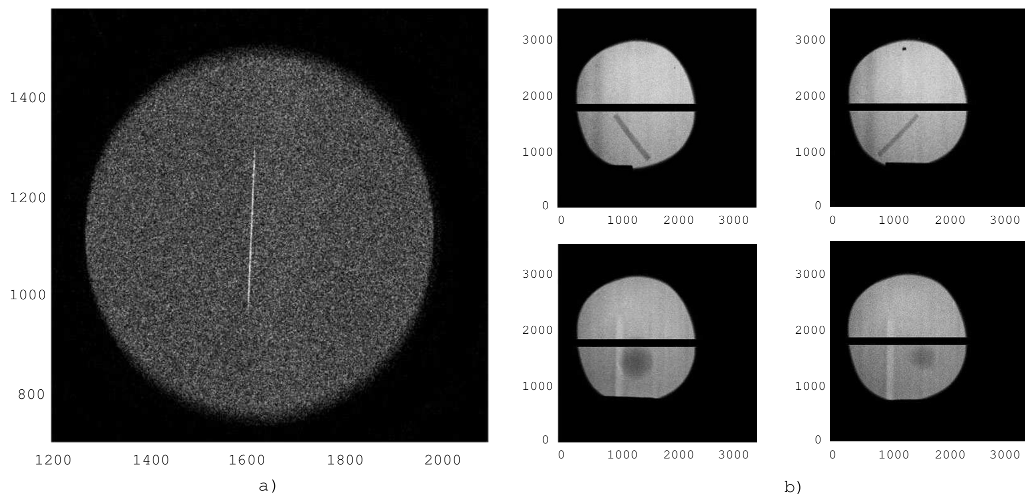

Figure 9: a) CCD image of a 5 μm wide slit machined into a stainless-steel target illuminated by 8 keV x rays. The CCD was 200 μm thick and was back illuminated and operated at -140°C. b) CCD images of an x-ray phantom consisting of various objects imbedded in 0.7 cm of paraffin and illuminated with 8 keV x rays. In all images a Be window defines the circular aperture.

Figure 10: Photographs of processing equipment at the LBNL MicroSystems Laboratory. a) Photograph of the projection aligner used to print patterns on 150 mm diameter wafers. b) Photograph of high-temperature furnaces used to oxidize silicon, deposit thin films, and anneal 150 mm diameter silicon wafers.

is the limited photon dynamic range. The number of electron hole pairs produced per incident x-ray photon is E_{photon}/E_i, where E_{photon} is the photon energy and E_i is the energy necessary to produce an electron-hole pair. The latter is approximately 3.65 eV [1], and therefore detection of high-energy x rays results in CCD full-well saturation for relatively small numbers of photons. For example, a 100,000 electron full well corresponds to about eighteen 20 keV photons. The ability to read out large format, fully depleted CCDs at high frame rates would significantly improve the dynamic range issue, and this is an area where one could benefit from the high level of readout-electronics integration that has been developed for HEP detector systems.

4. CCD fabrication

An important consideration in the development of fully depleted CCDs is the fabrication technology. We originally reported fully depleted CCDs that were entirely fabricated at LBNL on 100 mm diameter wafers in the MicroSystems Laboratory, a Class 10 clean-room [12]. More recently we have adopted a fabrication strategy in which the majority of the fabrication is done at a commercial CCD foundry, with the processing steps necessary for back-illumination done at LBNL [13]. In this case partially processed wafers from the foundry are thinned at a commercial vendor to the desired final thickness, and the backside in-situ doped (phosphorus) polycrystalline silicon layer is de-

posited on the wafers at LBNL. The remaining steps are contact lithography and etching, aluminum deposition, metal mask lithography and etching, sintering of contacts, and deposition of backside anti-reflecting coatings. These steps are done on non-standard thickness wafers, typically 200–250 μm thick, at the LBNL MicroSystems Laboratory. An advantage of this approach is that the CCDs are fabricated in batch mode at wafer level. Figure 10 shows some of the 150 mm wafer fabrication equipment used to process fully depleted CCDs at LBNL.

5. Summary

We have described fully depleted CCDs and compared them to the fully depleted p-i-n diode upon which they are derived from. Unique features of thick, fully depleted CCDs are enhanced red response, lack of fringing, controlled spatial resolution, and improved detection efficiency of x rays. Current efforts include development of high-voltage-compatible CCDs and continuing efforts in fabrication technology development.

Acknowledgments

The author wishes to thank Bill Kolbe, Jessamyn Fairfield, Armin Karcher, Kyle Dawson, Richard Stover, Mingzhi Wei, and Kirk Gilmore for CCD measurements, Guobin Wang and Nick Palaio for CCD fabrication, John Emes for CCD packaging, Don Groom for CCD modeling, Matthew Church, James Glossinger, and Howard Padmore for assistance with the x-ray measurements, and Natalie Roe and Chris Bebek for project oversight. This work was sponsored by the United States Department of Energy under contract No. DE-AC02-05CH11231. Kitt Peak National Observatory and the National Optical Astronomy Observatory are operated by the Association of Universities for Research in Astronomy, Inc. (AURA) under cooperative agreement with the National Science Foundation. The WIYN Observatory is a joint facility of the University of Wisconsin-Madison, Indiana University, Yale University, and the National Optical Astronomy Observatory.

References

[1] J.R. Janesick, *Scientific charge-coupled devices*, SPIE Press, Bellingham, WA, 2001.

[2] S.E. Holland, D.E. Groom, N.P. Palaio, R.J. Stover, and M. Wei, "Fully depleted, back-illuminated charge-coupled devices fabricated on high-resistivity silicon," *IEEE Trans. Elec. Dev.*, **50**, pp. 225–238, 2003.

[3] M.H. White, D.R. Lampe, F.C. Blaha, and I.G. Mack, "Characterization of surface channel CCD image arrays at low light levels," *IEEE J. Solid-State Cir.*, **9**, pp. 1–13, 1974.

[4] S. Holland, "Fabrication of detectors and transistors on high-resistivity silicon," *Nuclear Instrum. Methods in Physics Research A*, vol. 275, pp. 537-541, March 1989.

[5] Image courtesy of Nigel Sharp, Rich Reed, Dave Dryden, Dave Mills, Doug Williams, Charles Corson, Roger Lynds, and Arjun Dey, National Optical Astronomy Observatory, WIYN Observatory, and National Science Foundation.

[6] Data courtesy of Xiaohui Fan of the University of Arizona Astronomy Department and the Sloan Digital Sky Survey.

[7] S.E. Holland, N.W. Wang, and W.W. Moses, "Development of low noise, back-side illuminated silicon photodiode arrays," *IEEE Trans. Nucl. Sci.*, **44**, pp. 445–447, 1997.

[8] J.A. Fairfield *et al.*, "Improved spatial resolution in thick, fully depleted CCDs with enhanced red sensitivity," *IEEE Trans. Nucl. Sci.*, submitted for publication.

[9] R.H. Richter *et al.*, "Strip detector design for ATLAS and HERA-B using two-dimensional device simulation," *Nucl. Instr. Meth. A*, **377**, pp. 412–421, 1996.

[10] S.E. Holland *et al.*, "High-voltage-compatible, fully depleted CCDs," to be published, *Proc. of SPIE*, **6276**, 2006.

[11] National Institutes of Standards Physical Reference Data, http://www.physics.nist.gov/PhysRefData/XrayMassCoef/cover.html.

[12] S.E. Holland *et al.*, "A 200 × 200 CCD image sensor fabricated on high-resistivity silicon," in *IEDM Technical Digest*, pp. 911–914, 1996.

[13] C. J. Bebek *et al.*, "Development of fully depleted, back-illuminated charge coupled devices," *Proc. of SPIE*, **5499**, pp. 140–150, 2004.